

Cyclotron resonance of composite fermions with two and four flux quanta

I.V. Kukushkin^{a,c,*}, J.H. Smet^a, K. von Klitzing^a, W. Wegscheider^{b,d}

^aMax-Planck-Institut für Festkörperforschung, D-70569 Stuttgart, Germany

^bWalter Schottky Institut, Technische Universität München, D-85748 Garching, Germany

^cInstitute of Solid State Physics, RAS, Chernogolovka 142432, Russia

^dInstitut für Experimentelle und Angewandte Physik, Universität Regensburg, D-93040 Regensburg, Germany

Abstract

The application of quantum field theoretical methods to strongly interacting many-body problems has reaped rich rewards. Foremost, it has nurtured the quasi-particle notion. The introduction of suitable fictitious entities permits to cast otherwise notoriously difficult many-body systems in a single-particle form. We can then take the customary physical approach, using concepts and representations which formerly could only be applied to systems with weak interactions, and still capture the essential physics. A most notable recent example occurs in the conduction properties of a two-dimensional electron system, when exposed to a strong perpendicular magnetic field B . They are governed by electron–electron interactions, that bring about the Nobel prize winning fractional quantum Hall effect (FQHE) (Perspectives on Quantum Hall effects, Wiley, New York, 1996). Composite fermions (CFs), that do not experience the external magnetic field but a drastically reduced effective magnetic field B^* , were identified as opposite quasi-particles that simplify enormously the understanding of the FQHE (Phys. Today (2000) 39; Phys. Rev. Lett. 63 (1989) 199). They behave as legitimate particles with well-defined charge, spin and statistics (Phys. Rev. B 47 (1993) 7312; Composite Fermions, World Scientific, Singapore, 1998; Phys. Rev. Lett. 70 (1993) 2944; 75 (1995) 3926; 71 (1993) 3846; 72 (1994) 2065; 77 (1996) 2272). They precess, like electrons, along circular orbits, with a diameter determined by B^* rather than B , and with a frequency that is hard to predict, since the effective mass remains enigmatic. Ever since their prediction, the demonstration of enhanced absorption of a microwave field that resonates with the frequency of their circular motion was considered the ultimate experiment to unravel this issue. Here, we report the observation of this cyclotron resonance of CFs with two and four flux quanta and extract their effective mass.

© 2003 Elsevier B.V. All rights reserved.

PACS: 71.10.Pm; 78.40.Fy; 71.70.Di

Keywords: Fractional quantum Hall effect; Composite fermions; Cyclotron resonance; Effective mass

Composite fermions (CFs) are electrons dressed with two magnetic flux quanta (more generally an

even number of flux quanta), that point opposite to the externally applied magnetic field [2–4]. The attachment of a flux quantum to an electron is a rather natural way to minimize the energy of the two-dimensional electron system (2DES), since the associated vortex expels other electrons from its neighbourhood and results in a decrease of the repulsive interaction

* Corresponding author. Max-Planck-Institut für Festkörperforschung, D-70569 Stuttgart, Germany.

E-mail address: j.smet@fkf.mpg.de (J.H. Smet).

between the 2D electrons. If two flux quanta penetrate the 2DES per electron, i.e. if the lowest Landau level is half filled and the filling factor ν equals $\frac{1}{2}$, the external magnetic field is effectively compensated and a metallic state of these compound particles emerges [4]. This state can be characterized by a Fermi wave vector and Fermi energy. A deviation of the magnetic field from exact half filling results in the appearance of a non-zero effective magnetic field B^* , that quantizes the CF-motion and discretizes their energy spectrum into Landau levels. In this framework, the fractional quantum Hall effect (for a review, see [1]) is a manifestation of this Landau quantization and is equivalent to the integer quantum Hall effect of CFs. A variety of experimental observations [5–10] can be understood straightforwardly in semiclassical terms of nearly independent composite particles.

Since the kinetic energy of electrons is entirely quenched in the course of applying a B -field, the CF cyclotron mass is not a renormalized version of the electron conduction band mass, but must be generated entirely from electron–electron interactions [4]. The search of the CF cyclotron resonance requires substantial sophistication over conventional methods used to detect the electron cyclotron resonance, since Kohn’s theorem [11] must be outwitted. It states that in a translationally invariant system, radiation can only couple to the center-of-mass coordinate and cannot excite other internal degrees of freedom. Phenomena originating from electron–electron interactions will thus not be reflected in the absorption spectrum. An elegant way to bypass this theorem is to impose a periodic density modulation to break translational invariance. The non-zero wave vectors defined by the appropriately chosen modulation may then offer access to the cyclotron transitions of CFs, even though they are likely to remain very weak. Therefore, the development of an optical detection scheme, that boosts the sensitivity to resonant microwave absorption by up to two orders of magnitude in comparison with traditional techniques, was a prerequisite for our studies. Furthermore, we exploited to our benefit the accidental discovery that microwaves, already incident on the sample, set up a periodic modulation through the excitation of surface acoustic waves (SAW).

The development of an optical luminescence detection scheme [12] that boosts the sensitivity to resonant microwave absorption was a prerequisite for

our studies. Several high-quality GaAs/Al_{0.3}Ga_{0.7}As heterostructures, containing a single 30 nm wide quantum well, served the investigation. The embedded 2DES, with carrier densities and electron transport mobilities between $0.6\text{--}1.5 \times 10^{11}/\text{cm}^2$ and $3\text{--}5 \times 10^6 \text{ cm}^2/\text{V s}$ respectively, were patterned into disks with a diameter of 1 mm [12]. The samples were placed near the end of a 16- or 8-mm short-circuited waveguide in the electric field maximum of the microwave excitation inside a He³ cryostat with a 12 T magnet. The frequency intervals 10–20 and 27–40 GHz were covered and the microwave power at the waveguide entrance was varied between 10 nW and 200 μW . Luminescence spectra *with* and *without* microwave excitation were recorded consecutively by using a CCD-camera, a double-grating spectrometer that provides a spectral resolution of 0.03 meV, and a stabilized semiconductor laser operating at a wavelength of 750 nm and approximately 100 μW of microwave power. The differential luminescence spectrum is obtained (see Fig. 1) when subtracting both luminescence spectra. To improve signal-to-noise ratio, the same procedure was repeated N times ($N = 2\text{--}20$). Subsequently, we integrated the absolute value of the averaged differential spectrum over the entire spectral range and hereafter refer to the value of this integral as *the microwave absorption amplitude*. The same procedure is then repeated for different values of B . This technique offers pre-eminent sensitivity as attested by our ability to observe the electron cyclotron resonance at microwave levels below 10 nW. To establish trustworthiness in this unconventional scheme, we apply it to the well-known case of the electron cyclotron resonance $\omega_{\text{cr}} = eB/m^*$, with m^* the effective mass of GaAs ($0.067 m_0$). Due to its limited size, the sample also supports a dimensional plasma mode with a frequency ω_p , that depends on both the density n_{2D} and diameter d of the sample, according to $\omega_p^2 = 3\pi^2 n_{2D} e^2 / (2m^* \epsilon_{\text{eff}} d)$. The plasma and cyclotron mode hybridize and the resulting resonance frequency of the upper dimensional magnetoplasma-cyclotron mode ω_{DMR} equals $\omega_{\text{cr}}/2 + [\omega_p^2 + (\omega_{\text{cr}}/2)^2]^{1/2}$ [12,13]. As it is clear from Figs. 2–3 the optical method indeed recovers this mode. A comparison with the theoretical expression for ω_{DMR} yields excellent agreement. No fitting is required, since the density can be independently extracted from the luminescence at higher B -fields, where Landau

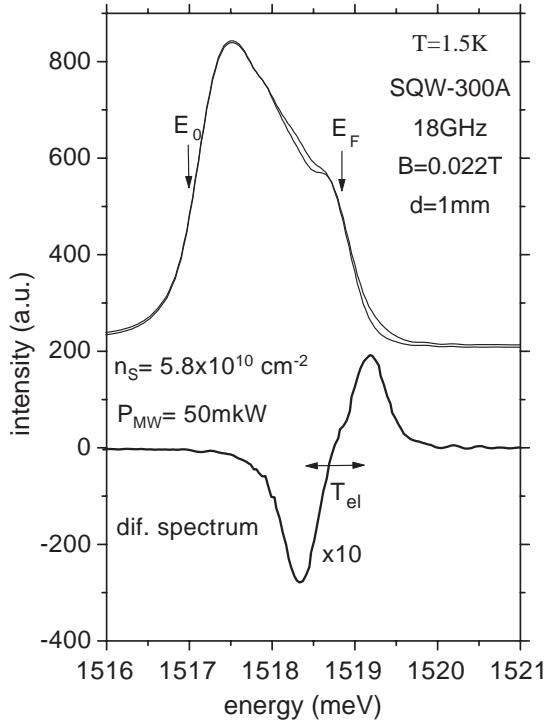


Fig. 1. Illustration of the optical scheme to detect resonant microwave absorption for the electron cyclotron-magnetoplasmon hybrid mode at low B -fields. Luminescence spectrum in the presence of (dotted line) and without (solid line) a $50 \mu\text{W}$ microwave excitation of 18 GHz obtained on a disk-shaped 2DES with a diameter of 1 mm and carrier density $n_s = 5.8 \times 10^{10}/\text{cm}^2$ at a magnetic field $B = 22 \text{ mT}$. In the vicinity of the Fermi energy E_F the spectrum is affected significantly under resonant microwave excitation due to heating. The dashed line represents the differential luminescence spectrum. The integration of its absolute value across the entire spectral range yields the microwave absorption amplitude. The width of the differential spectrum reflects the increased electron temperature T_e .

levels can be resolved. At sufficiently low density, the influence of ω_p on the hybrid mode drops and one recovers at large enough B the anticipated $\omega_{\text{cr}} = eB/m^*$ -dependence. Further details of the electron cyclotron resonance are discussed elsewhere [12]. Additional support for the validity of the detection method comes from a comparison with the measurements based on the conventional approach using a bolometer (see Fig. 2). Not only does one find the same resonance position, but also the same line shape. The only difference is the improved signal-to-noise ratio (30–100 times) for the optical detection scheme.

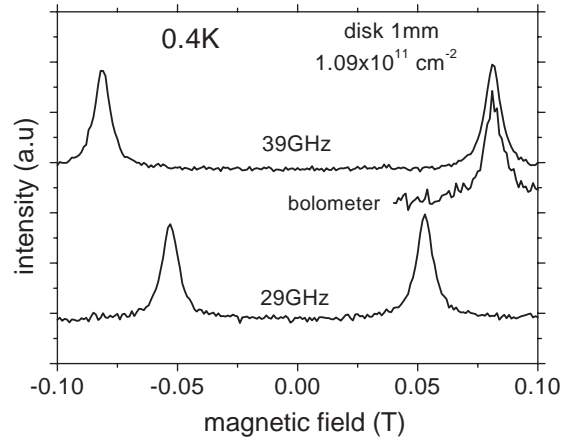


Fig. 2. The microwave absorption amplitude at 29 and 39 GHz as a function of B -field by recording differential luminescence spectra for 1 mT field increments at $n_s = 1.09 \times 10^{11}/\text{cm}^2$. The peaks, symmetrically arranged around zero field, are identified as the dimensional magnetoplasma-cyclotron hybrid mode. Conventional bolometer measurements are also shown.

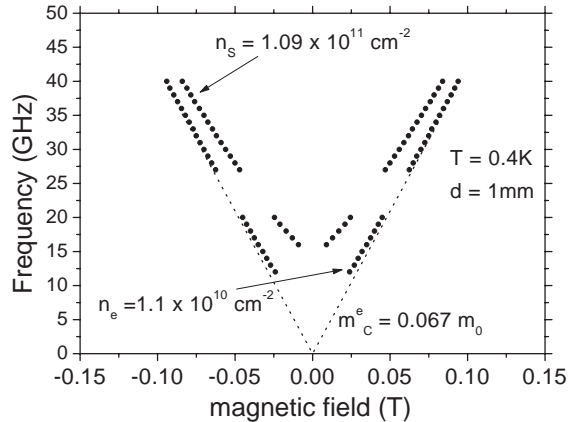


Fig. 3. Resonance position for $n_s = 1.09 \times 10^{11}$ and $1.1 \times 10^{10}/\text{cm}^2$ as a function of incident microwave frequency. The intervals 10–20 and 27–40 GHz were covered. The dashed lines represent the theoretical dependence of the hybrid dimensional magnetoplasma-cyclotron resonance. The dotted line corresponds to the cyclotron mode only.

Disorder and the finite dimensions of the sample, in principle, suffice to break translational invariance as attested by the interaction of the cyclotron and dimensional plasma mode. However, they provide access to internal degrees of freedom other than the

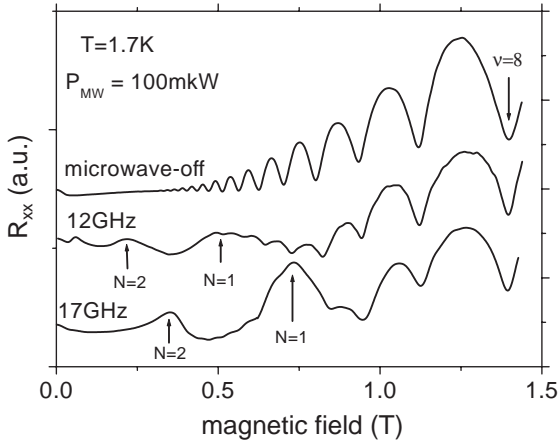


Fig. 4. Magnetotransport data without (top curve) and under 100 μ W of microwave radiation at 12 (middle curve) and 17 GHz (bottom curve). Curves are offset for clarity. Besides the well-known Shubnikov–de Haas oscillations, additional magnetoresistance oscillations appear under microwave radiation. They are commonly observed in 2DEs on which a static periodic modulation of the density has been imposed.

center-of-mass motion of the electrons either at poorly defined wave vectors or too small a wave vector for appropriate sample sizes. Therefore, the imposition of an additional periodic density modulation, that introduces larger and well-defined wave vectors to circumvent Kohn's theorem, is desirable. Transport experiments in the Hall bar geometry disclosed that additional processing is not required, since the microwaves, already incident on the sample, concomitantly induces a periodic modulation at sufficiently high power. A clear signature is the appearance of commensurability oscillations in the magneto-resistance due to the interplay between the B -dependent cyclotron radius of electrons and the length scale imposed by the modulation [14]. Examples are displayed in Fig. 4 and resemble the data in Ref. [15], where the modulation is produced with the help of SAW-transducers. Here, the following scenario is conceivable. Owing to the piezoelectric properties of the $\text{Al}_x\text{Ga}_{1-x}\text{As}$ -crystal, the radiation is partly transformed into SAW with opposite momentum, so that both energy and momentum are conserved. Reflection from cleaved boundaries of the sample then produces a standing wave with a periodicity determined by the sound wavelength. The involvement of sound waves can be deduced from trans-

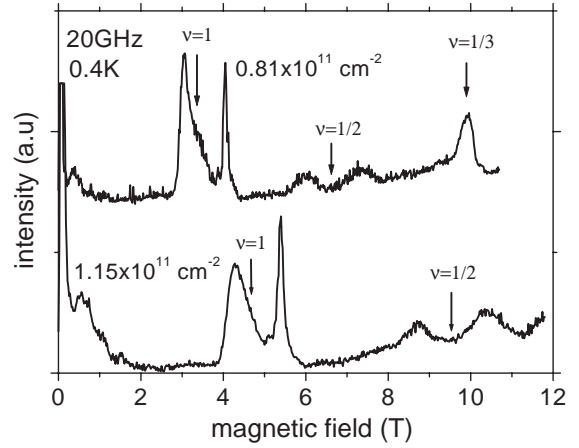


Fig. 5. Microwave absorption amplitude at high magnetic fields for $n_s = 0.81 \times 10^{11}$ and $1.15 \times 10^{11}/\text{cm}^2$ and frequency of 20 GHz. The response near $\nu = 1$ and $\frac{1}{3}$ does not shift with frequency.

port data, since from the minima we expect the modulation period to be approximately 200 and 250 nm for frequencies of 17 and 12 GHz, respectively. The ratio of this period to the sound wavelength at these frequencies is 1.12 and 1.15. More detailed investigations of transport properties of 2D-electrons under microwave irradiation which illustrate transformation of microwaves into surface acoustical waves are published in Ref. [16].

Fig. 5 depicts the microwave absorption amplitude up to high B -fields. Apart from the strong dimensional magnetoplasma-cyclotron resonance signal at low B -field discussed above, several peaks, that scale with a variation of the density, emerge near filling $1, \frac{1}{2}$ and $\frac{1}{3}$. Those peak positions associated with $\nu = 1$ and $\frac{1}{3}$ remain fixed when tuning the microwave frequency and are ascribed to heating induced by non-resonant absorption of microwave power. In contrast, the weak maxima surrounding filling $\frac{1}{2}$ readily respond to a change in frequency as illustrated in Fig. 6. They are symmetrically arranged around half filling and their splitting grows with frequency. The B -dependence is summarized in Fig. 7 for two densities. To underline the symmetry, B^* was chosen as the abscissa. The linear relationship between frequency and field extrapolates to zero at vanishing B^* . We do not expect a deviation at small B^* due to a plasma-like contribution as in Fig. 3. Excitations for the $\frac{1}{3}, \frac{2}{3}, \frac{3}{7}$ and other

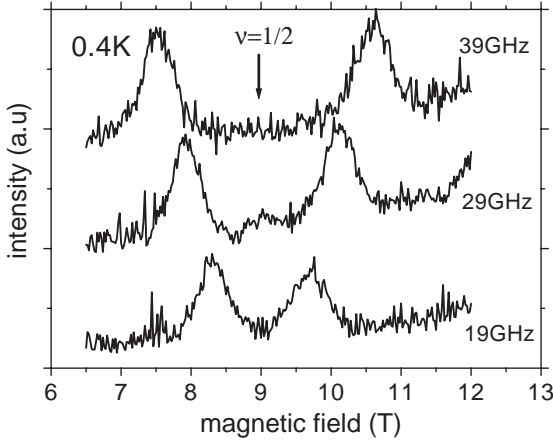


Fig. 6. Microwave absorption amplitude in the vicinity of $\nu = \frac{1}{2}$ (20 mT step size) at three different frequencies and $n_s = 1.09 \times 10^{11}/\text{cm}^2$. The peak values are nearly two orders of magnitude weaker and considerably wider (about 30–50 times) than those due to the electron cyclotron resonance.

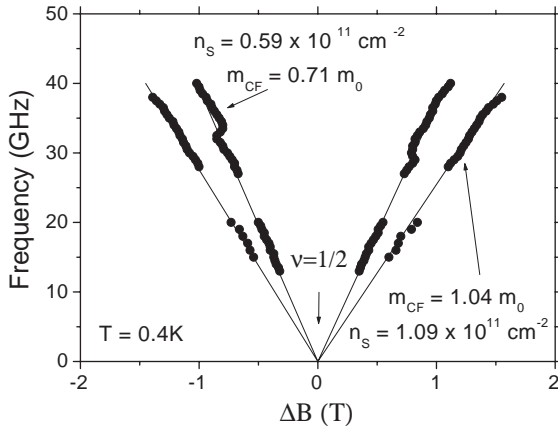


Fig. 7. Position of the CF cyclotron mode as a function of the effective magnetic field $B^* = B - 2n_s F_0$ (F_0 is the elementary flux quantum) for $n_s = 1.09 \times 10^{11}/\text{cm}^2$ (circles) and $n_s = 0.59 \times 10^{11}/\text{cm}^2$ (squares). The CF effective mass equals $1.04 m_0$ and $0.71 m_0$, respectively. The resonances remain visible even if the 2DES condenses in the gapfull fractional quantum Hall states at filling factors $\frac{3}{5}$ and $\frac{3}{7}$.

fractional quantum Hall states exhibit in numerical simulations no magnetoplasmon-like linear contribution to the dispersion at small values of k [17]. We conclude that the resonance in Fig. 6 is the long searched for cyclotron resonance of CFs. Geometric resonances

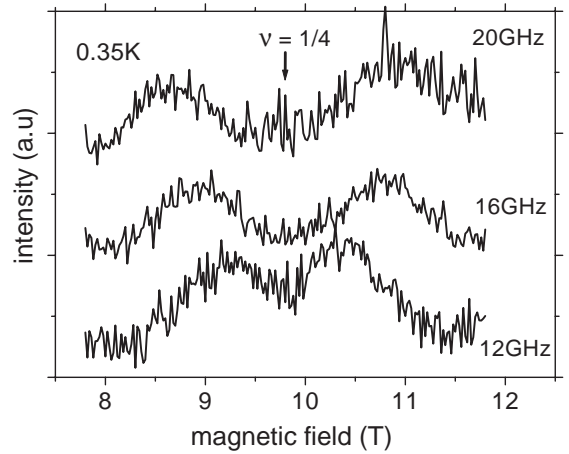


Fig. 8. Microwave absorption amplitude in the vicinity of $\nu = \frac{1}{4}$ (20 mT step size) at three different frequencies and $n_s = 0.59 \times 10^{11}/\text{cm}^2$.

(GR), as they occur in transport at low fields due to the density modulation (Fig. 4), are excluded as an alternative interpretation for the observed features on the following grounds: (I) In the optical data, only the electron cyclotron resonance peak is observed. Contrary to optical quantities, transport is also sensitive to semi-classical phenomena unrelated to changes in the density of states. (II) Even if the 2DES condenses in a FQHE-state and the chemical potential is located in a gap, the resonance peaks surrounding $\nu = \frac{1}{2}$ occur (Fig. 7). Commensurability effects are not observable in this regime. (III) The observation of GRs requires that the density modulation is temporally static on the time scale with which CFs execute their cyclotron orbit. For electrons at low fields this condition is met and accordingly *transport* displays GRs. For the anticipated enhanced mass of CFs, this condition is violated. (IV) Analogous resonance peaks were also detected for the higher order CFs around $\nu = \frac{1}{4}$ which are shown in Fig. 8. Since at fixed electron density the CF metallic state is characterized by the same Fermi wave vector, GRs would show up at the same distance from $\nu = \frac{1}{4}$ as they do at $\nu = \frac{1}{2}$. As it is obvious from Fig. 9 the observed peaks are located at different positions rendering a commensurability picture untenable.

In contrast to electron cyclotron resonance, the intensity of the CF cyclotron resonance is a strong non-linear function of microwave power (Fig. 10).

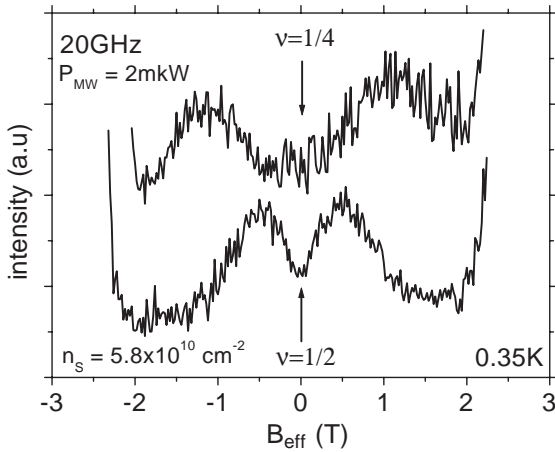


Fig. 9. Comparison of peak positions of cyclotron resonances measured at fixed electron density $n_s = 0.59 \times 10^{11}/\text{cm}^2$ for CFs with two and four flux quanta.

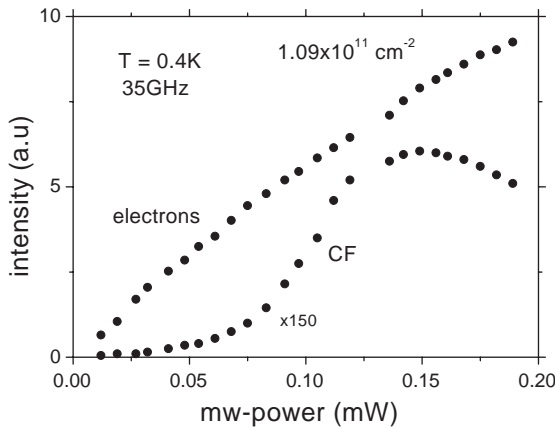


Fig. 10. Incident microwave power dependence of the amplitude at the cyclotron resonance measured for electrons and for CFs.

Moreover, its observability only at high power correlates with the first appearance of commensurability oscillations. The drop in intensity at even higher power is most probably due to heating. The intensity diminishes to zero at temperatures above 0.7 K, whereas the electron cyclotron resonance persists up to $T > 2$ K. The slope of the CF cyclotron frequency as a function of B^* in Fig. 6 defines the cyclotron mass $m_{\text{cr}}^{\text{cf}}$. This mass is set by the electron–electron interaction scale, so that a square root behaviour on

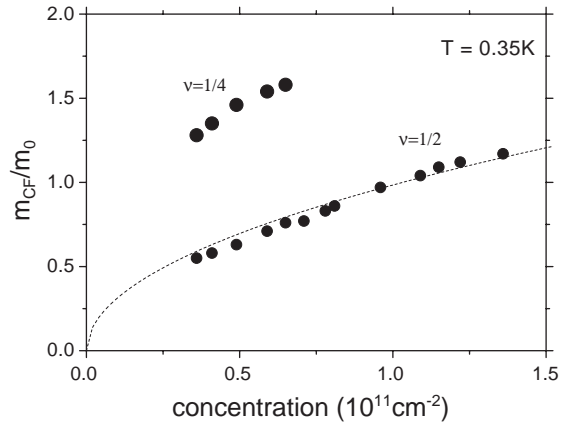


Fig. 11. Density dependence of the CF effective mass measured both for $\nu = \frac{1}{2}$ and $\frac{1}{4}$. The dashed line is a square root fit to the data.

density or B -field is forecasted from a straightforward dimensional analysis [4]. Numerical calculations predict $m_{\text{cr}}^{\text{cf}}/m_0 = 0.079 (B[T])^{1/2}$ for an ideal 2DES, not including Landau level mixing or finite width contributions [18]. The data, shown in Fig. 11, confirm qualitatively the strong enhancement in comparison with the electron mass (more than 10 times), however a fit to the square root dependence requires a prefactor that is four times larger. It is also clear from Fig. 11 that attachment of additional flux quanta to electron results to further enhancement of the mass of CFs. Note that previously reported mass values based on activation energy gap measurements [19,20] must be distinguished from the cyclotron mass. The former corresponds to the limit of infinite momentum, whereas here k approaches zero. Moreover, activation gaps can only be extracted at well-developed fractional quantum Hall states and their accurate determination suffers from disorder induced broadening. These and other limitations have been discussed in Ref. [19] for example. The technique discussed here can be performed at arbitrary filling factors.

In summary, the fortuitous breaking of translational invariance induced by the microwave irradiation combined with the virtues of an optical detection scheme for resonant absorption has enabled to unveil the cyclotron resonance frequency of CFs with two and four flux quanta and to measure the corresponding cyclotron masses.

Acknowledgements

Partial support by the Max–Planck and Humboldt Research Award, the Russian Fund of Fundamental Research, INTAS, the German Ministry of Science and Education and the German Physical Society is gratefully acknowledged.

References

- [1] S. Das Sarma, A. Pinczuk (Eds.), *Perspectives on Quantum Hall Effects*, Wiley, New York, 1996.
- [2] J.K. Jain, *Phys. Today* 53 (2000) 39.
- [3] J.K. Jain, *Phys. Rev. Lett.* 63 (1989) 199.
- [4] B.I. Halperin, P.A. Lee, N. Read, *Phys. Rev. B* 47 (1993) 7312.
- [5] O. Heinonen (Ed.), *Composite Fermions*, World Scientific, Singapore, 1998.
- [6] R.R. Du, et al., *Phys. Rev. Lett.* 70 (1993) 2944.
- [7] R.R. Du, et al., *Phys. Rev. Lett.* 75 (1995) 3926.
- [8] R.L. Willett, et al., *Phys. Rev. Lett.* 71 (1993) 3846.
- [9] V.J. Goldman, et al., *Phys. Rev. Lett.* 72 (1994) 2065.
- [10] J.H. Smet, et al., *Phys. Rev. Lett.* 77 (1996) 2272.
- [11] W. Kohn, *Phys. Rev.* 123 (1961) 1242.
- [12] S.I. Gubarev, et al., *JETP Lett.* 72 (2000) 324.
- [13] S.J. Allen, et al., *Phys. Rev. B* 28 (1983) 4875.
- [14] R.R. Gerhardts, et al., *Phys. Rev. Lett.* 62 (1989) 1173.
- [15] J.M. Shilton, et al., *Phys. Rev. B* 51 (1995) 14770.
- [16] I.V. Kukushkin, et al., *Phys. Rev. B* 66 (2002) 121306(R).
- [17] J.K. Jain, R.K. Kamilla, Composite fermions: particles of the lowest Landau level, in: O. Heinonen (Ed.), *Composite Fermions*, World Scientific, Singapore, 1998, pp. 1–80.
- [18] K. Park, J.K. Jain, *Phys. Rev. Lett.* 80 (1998) 4237.
- [19] R.R. Du, et al., *Phys. Rev. Lett.* 70 (1993) 2944.
- [20] R.L. Willett, Composite fermions—experimental findings, in: O. Heinonen (Ed.), *Composite Fermions*, World Scientific, Singapore, 1998, p. 349.